J. Plasma Physics (2010), *vol.* 76, *part* 5, *pp.* 735–747.
doi:10.1017/S0022377809990419

Anisotropies in a charged particle beam

WILSON SIMEONI, JR

Instituto de Física, Universidade Federal do Rio Grande do Sul,
Caixa Postal 15051, 91501-970, Porto Alegre, RS, Brazil
(wsjr@if.ufrgs.br)

(Received 5 June 2009 and in revised form 17 October 2009, first published online 16 December 2009)

Abstract. This paper examines the anisotropies of a charged particle beam moving into a linear focusing channel. Considering a high-intensity ion beam in space-charge-dominated regime and large mismatched root mean square (RMS) initial beam size, a fast increase in spatial beam anisotropy is observed. Calculations presented here are strong evidence that this anisotropy is responsible for the beam's equipartition. It is shown that particle–particle resonances and wave-particle resonances lead to anisotropization of the beam, *i.e.* both the envelope and emittance ratios different from unity. It indicates that this anisotropy is responsible for the beam's equipartitioning and suggest that the beam remains equipartitioned even when exhibiting a macroscopic anisotropy, which is characterized by the following properties: the development of an elliptical shape with increasing size along one axis, the presence of a coupling between transversal emittances and halo formation along a preferential direction.

1. Introduction

It is known that nonlinear space-charge forces in space-charge-dominated ion beams are responsible for the formation of filamentation pattern, in the beam spatial distribution resulting in a 2-component beam consisting of an inner core and an outer halo [1–4]. When this core is mismatched in a uniform linear focusing channel, the envelope oscillates and the particles, represented by single test particles, oscillate about and through the core. This mechanism is called particle-core model since it consider test particles initially located outside the core. The test particles execute betatron oscillations under the influence of space-charge field induced by the oscillating core, and exhibit various nonlinear behaviors, including parametric resonance. A number of numerical analysis and macroparticle simulations suggested that the 2:1 parametric resonance between test particle oscillation and breathing core oscillation is likely the main cause of halo formation [5–11].

Space-charge-induced coupling between different degrees of freedom can be responsible for emittance growth or transfer of emittance from one phase plane to another. In an analytical single-particle analysis Montague [12] pointed out that the space-charge driven fourth-order difference resonance may lead to emittance coupling. The theory of space-charge coupling resonances has been studied most thoroughly by Hofmann using Vlasov equation [13]. Intrinsic coupling resonances are an important consideration to be taken into account in linear acelerators, and may also be of interest in rings when the tune separation is small [14]. The coupling

resonances driven by the beam's space-charge fields depend only on the relative emittances or average focusing strengths. In anisotropic beams, the emittance and/or external focusing force strength are different in the two transversale directions. Effects of anisotropic cores on halo dynamics have been studied by Ikegami [15].

Most of the halo studies so far have considered round beams with axisymmetric focusing. Some new aspects caused by anisotropy demonstrate an influence of the mismatch on halo size [16, 17]. In fact, mismatch oscillations can drive particles into the halo as the result of resonant interaction between these particles and the mismatch mode [6]. So far only second-order round beams have been considered as possible mismatch modes: the influence of anisotropic on second and higher order mismatch modes is expected to be an important factor for halo formation.

Previous work has been done in this direction by means of nonlinear analysis of the beam's transport considering non-axisymmetric perturbations [18]. It was shown that large-amplitude breathing oscillations of an initially round beam couple nonlinearly to quadrupole-like oscillations. Such that the energy excess, which is initially constrained to the axisymmetric breathing oscillation, is allowed to flow back and forth between breathing and quadrupole-like oscillations. In this case, the beam develops an elliptical shape with an increase in its size along one direction as the beam is transported, representing a highly nonlinear phenomenon that occurs for large mismatch amplitudes on the order of 100% [19].

This paper aims at quantifying the relationship between the anisotropy of the beam and the equipartition and how this relationship is driven by anisotropic processes. Analyzing the effect of the particle–particle resonances and wave-particle resonances in the beam, it is shown that these resonances lead to the anisotropy of the beam, that is, both the envelope ratio and the emittance ratio are different from unity. The conjecture presented here is that this anisotropy is responsible for the beam's equipartitioning.

This paper is organized as follows. In Sec. 2 the models equations are derived, while Sec. 3 describes the examination of the anisotropies in the ion beam in a linear focusing channel. Finally, Sec. 4 discusses implications and possible extensions of our results.

2. The model equations

An axially long unbunched beam of ions of charge q and mass m propagating with average axial velocity $\beta_b c\hat{\mathbf{e}}_z$ along an uniform solenoidal focusing field $\mathbf{B}(\mathbf{x}) = B_z\hat{\mathbf{e}}_z$ are considered. Self-field interactions are regarded as electrostatic. The parameters c and $\gamma_b = 1/\sqrt{1-\beta_b^2}$ are the speed of light *in vacuo* and the relativistic factor, respectively. We assume that the beam has an elliptical cross-section centered at $x = y = 0$ and a vanishing canonical angular momentum $P_\theta \equiv \langle xy' - yx' \rangle = 0$, where x and y are the positions of the beam's particles. We consider a beam with a non-uniform density in a space-charge-dominated regime with a initial emittance such that $\epsilon_x = \epsilon_y$.

As demonstrated by Sacherer [20] and Lapostolle [19], the envelope equations for a continuous beam are not restricted to uniformly charged beams, but are equally valid for any charge distribution with elliptical symmetry, provided that the beam boundary and the emittance are defined by root mean square (RMS) values. Thus, we consider the parabolic density $n_b = 2N_b/\pi r_x r_y[1 - x^2/r_x^2 - y^2/r_x^2]$, where

https://doi.org/10.1017/S0022377809990419 Published online by Cambridge University Press

$r_x = \sqrt{6\langle x^2\rangle}$ and $r_y = \sqrt{6\langle y^2\rangle}$ are the ellipse semi-axis RMS. The parameter N_b is the axial line density.

For a parabolic density $n(x, y)$, the Poisson equation $\nabla_\perp^2 \phi = -qn/\varepsilon_0$, ε_0 being the permittivity of free space, provides the basis to obtain the space-charge field component (assuming a paraxial approximation). The density is assumed to be zero outside of the ellipse and the solution has been given by Lapostolle [21]. The electrostatic potentials inside the beam (ϕ_{in}) and outside the beam (ϕ_{out}) are given by

$$\phi_{in} = \frac{2qN_b}{\pi\varepsilon_o}\left\{\frac{x^2}{r_x(r_x+r_y)} + \frac{y^2}{r_y(r_x+r_y)} - x^4\left[\frac{2r_x+r_y}{3r_x^3(r_x+r_y)^2}\right]\right.$$
$$\left. - y^4\left[\frac{2r_y+r_x}{3r_y^3(r_x+r_y)^2}\right] - x^2y^2\left[\frac{1}{r_xr_y(r_x+r_y)^2}\right]\right\}, \tag{2.1}$$

$$\phi_{out} = \frac{q}{4\pi\varepsilon_0}\log\left[y^2 + x^2 + \lambda + \sqrt{2}y\Lambda^+ + \sqrt{2}x\Lambda^-\right]$$
$$+ \frac{q}{2\pi\varepsilon_0\lambda^2}\left[y^2 - x^2 - \frac{y}{\sqrt{2}}\Lambda^+ + \frac{x}{\sqrt{2}}\Lambda^-\right], \tag{2.2}$$

where $\lambda = r_x^2 - r_y^2$, $\Lambda = \sqrt{(x^2 - y^2 - \lambda^2)^2 + 4x^2y^2}$ and $\Lambda^\pm = \sqrt{\Lambda \pm (x^2 - y^2 \mp \lambda^2)}$.

The transverse orbit $x(s)$ and $y(s)$ of a beam particle satisfy the paraxial equations of motion:

$$x'' + \kappa_0^2 x = \frac{-q}{m\gamma_b\beta_b^2c^2}\frac{\partial\phi}{\partial x}, \tag{2.3}$$

$$y'' + \kappa_0^2 y = \frac{-q}{m\gamma_b\beta_b^2c^2}\frac{\partial\phi}{\partial y}, \tag{2.4}$$

where s is the axial coordinate of the beam and the primes denote derivatives with respect to s. The parameter $\kappa_0 = qB_z/2\gamma_b\beta_bmc^2$ is the vacuum phase advance per unit of axial length and it measures the focusing field strength.

The envelope of the beam is an elliptical cross-section with RMS radii r_j (henceforth, j ranges over both x and y) that obey the RMS–KV envelope equations [22]:

$$r_j'' + \kappa_0^2 r_j - \frac{2K}{r_x + r_y} - \frac{\epsilon_j^2}{r_j^3} = 0. \tag{2.5}$$

Here, $K = q^2N_b/\pi^2\varepsilon_0\gamma_b^3\beta_b^2mc^2$ is the dimensionless perveance of the beam and $\epsilon_j = \sqrt{\langle j^2\rangle\langle j'^2\rangle - \langle jj'\rangle^2}$ is RMS emittance of the beam along the j plane.

ϵ_j can be calculated analytically following a model proposed to Lapostolle et al. [23] for nonlinear space-charge forces, where these forces cause a change in the momentum components, *i.e.* the product of the force and the amount of time over which the force acts. The force depends on the spatial distribution of the particles, and particle coordinates on which the force acts. In general, these changes in the momentum components modify the phase-space distribution of the particles. From the electrostatic potential, the transverse momentum impulse can be calculated and this results in a new phase-space distribution and new RMS emittance [24, 25]. For example, in the x plane the change in the momentum component is $\triangle p_x = qE_xL/v_b$, where $E_x = \partial\phi^{in}/\partial x$ is the electric field, v_b is the beam velocity, and L is the length

https://doi.org/10.1017/S0022377809990419 Published online by Cambridge University Press

of the drift space. The impulse can also be expressed as a change in the divergence angle, given non-relativistically in the paraxial approximation by $\triangle x^{'} = qE_xL/m_bv_b^2$. If the second momentas of the particle distribution can be evaluated from the expression for x and $x^{'}$, the RMS emittance can be obtained. Assuming fixed positions, with divergence $x^{'} = x/r_x + qE_xL/m_bv_b^2$, the RMS emittance for parabolic density yields [26]:

$$\epsilon_x = \frac{1}{90}\sqrt{15}KL\left\{\frac{\left(\frac{r_x}{r_y}\right)^2\left[5\left(\frac{r_x}{r_y}\right)^2 + 2\frac{r_x}{r_y} + 5\right]}{\left(1+\frac{r_x}{r_y}\right)^4}\right\}^{1/2}, \tag{2.6}$$

$$\epsilon_y = \frac{1}{90}\sqrt{15}KL\left\{\frac{\left(\frac{r_y}{r_x}\right)^2\left[5\left(\frac{r_y}{r_x}\right)^2 + 2\frac{r_y}{r_x} + 5\right]}{\left(1+\frac{r_y}{r_x}\right)^4}\right\}^{1/2}. \tag{2.7}$$

One can see that the emittance depends on the beam's perveance K and on the ratio of the beam semi-axes. The first term corresponds to the filamentation effect caused by the fourth-order term in the electrostatic potential. The second term comes from the coupling, i.e the x component dependence of the potential on the y coordinate, which produces the spreading of the initial filamentation. The last term is a cross term between the filamentation term and the coupling term.

The KV distribution has been frequently taken as a theoretical basis of the particle-core model since this implies that the space-charge forces are linear. However, there is little doubt that intense beams are dominated by nonlinear interactions. It may thus be reasonable to develop alternative particle-core models with nonlinear core potentials. From this point of view, we propose here a parabolic core under a simplifying assumption. The core is described by the RMS envelope (2.5) and the halo particles are modeled using test particles. These are subjected to the external force and the time-dependent nonlinear space-charge force associated with the parabolic core. We assume that the parabolic-type density is roughly maintained even for a mismatched beam, thus the spatial distribution is assumed to remain unchanged as the beam propagates. The test particles do not affect the motion of the core [27], which are described by (2.3) and (2.4), with the electrostatic potentials ϕ_{in} and ϕ_{out}.

3. Ion beam anisotropies

It is easy to verify that there is a particular solution of the envelope (2.5) for which $r_j(s) = r_{b0} = [(K + (K^2 + 4\kappa_0^2\eta^2)^{1/2})/2\kappa_0^2]^{1/2}$, where $\eta = \epsilon_x/\epsilon_y$ is the emittance ratio. This corresponds to the so called matched solution for which a circular beam of radius r_{b0} preserves its shape throughout the transport along the focusing channel. Then, we transform the equations to a dimensionless form introducing the following dimensionless variables and parameters: $\tau = \kappa_0 s$ for the independent variable, $\tilde{r_x} = \sqrt{\kappa_0/\epsilon_y}r_x$ and $\tilde{r_y} = \sqrt{\kappa_0/\epsilon_y}r_y$ for envelope beam, $\tilde{x} = \sqrt{\kappa_0/\epsilon_y}x$ and $\tilde{y} = \sqrt{\kappa_0/\epsilon_y}y$ for test particle, and $\tilde{K} = K/\epsilon_y\kappa_0$ for the scaled space-charge perveance. We introduce here the following anisotropy variables: the emittance ratio $\eta = \epsilon_x/\epsilon_y$; the ratio of the envelope beam $\chi = r_x/r_y$; the mismatch factor is $\nu = r_x/r_{b0} = r_y/r_{b0}$.

https://doi.org/10.1017/S0022377809990419 Published online by Cambridge University Press

The beam is initially set in a state with $\tilde{K} = 3$, $\kappa_0 = 1$, $v = 2.4$, $L = 2$ $r_{j0} = vr_{b0}$, $r_{x0} = r_{y0}$ and $\eta = 1$. The envelope (2.5) up to $s = 50$ are then integrated and the corresponding evolution of the RMS emittances $\{\epsilon_j\}$ is calculated through (2.6) and (2.7). It is convenient to introduce new canonical variables defined as $X_s = (r_x + r_y)/2$ and $X_a = (r_x - r_y)/2$, in order to analyze the oscillation modes of the beam. Note that X_s describes oscillations where $r_x(s)$ and $r_y(s)$ oscillate in phase: the breathing modes. The variable X_a describes oscillations where $r_x(s)$ and $r_y(s)$ oscillate with opposite phase: the quadrupole modes [18].

One can readily see in Fig. 1 that the beam develops an elliptical shape that increases its size along the x direction. This effect follows the large initial mismatch of the beam that couples to the previously described oscillation modes. This leads to the perturbation of the nonlinear space-charge force and therefore induces the coupling between different degrees of freedom and core–core resonances [16, 28]. Real core–core resonances [13] are observed for RMS mismatched beams fulfilling internal resonance conditions between the planes. The mismatched size RMS beam is the energy excess given to the system. In general, this excess appears as energy oscillations in the degrees of freedom of the system. Space-charge coupling of these degrees of freedom causes a resonance leading to energy transfer between the relevant degrees of freedom. In Fig. 1 (bottom), it is shown that there is an increase of the oscillation amplitude of the modes, featuring a resonance between the breathing and the quadrupole mode. This resonance was analyzed through the numerical calculations (Fourier analysis) of the dimensionless frequencies related breathing and the quadrupole oscillation modes. The frequencies associated with the breathing or the quadrupole mode correspond to the maximum in the Fourier transform. Details about the implementation of the Fourier transform can be found in [29]. The breathing mode and quadrupole mode frequencies are $\omega_{X_s} = \omega_{X_a} = 2.01334$.

In the emittance dynamics analysis of (2.6) and (2.7), the initial transversal emittances are set to $\epsilon_{x0} = \epsilon_{y0} = 0.22360$ [26]. The corresponding results for the emittance dynamics are shown in Fig. 2. Here one can observe that the difference between resonances results in a coupling of the emittances, which are driven by the space charge [12, 30, 31]. This coupling is characterized by an emittance exchange between both directions. Space-charge affects the net forces as seen by the individual particles in such a way that they become nonlinear and dependent on the density distribution of the beam. Furthermore, emittance exchange requires a resonant coupling, which can take place only if an intrinsic resonance relationship is fulfilled. In this scenario, a simplified approach consists of a single-particle resonance difference where the condition $l\omega_x - m\omega_y = 0$ is fulfilled (l and m are integer numbers), as suggested in [32]. In this case, ω_x and ω_y are the single-particle frequency along the x and y directions, respectively. The motion is always bounded in both x and y directions. This emittance coupling is an expression of the exchange of energy between these directions, which is a common feature in linearly coupled systems $l = m = 1$. In this work, the dimensionless frequencies ω_x and ω_y of 2500 test particles by were numerically computed by means of the Fourier transform. Following, test particles were released along the x- and y-axis of the beam at positions constrained between $0.01r_j$ and $0.7r_j$ spaced by $0.0004r_j$ along both j directions – x and y. It was observed that 2455 particles acquired the same frequency $\omega_x = \omega_y = 1.05461$ in both directions. Thus it can be argued that these 2455 test particles are subject to the resonance condition $\omega_x - \omega_y = 0$. These results are illustrated by the histogram in Fig. 4. Since a large fraction of test particles in resonance gives rise to

https://doi.org/10.1017/S0022377809990419 Published online by Cambridge University Press

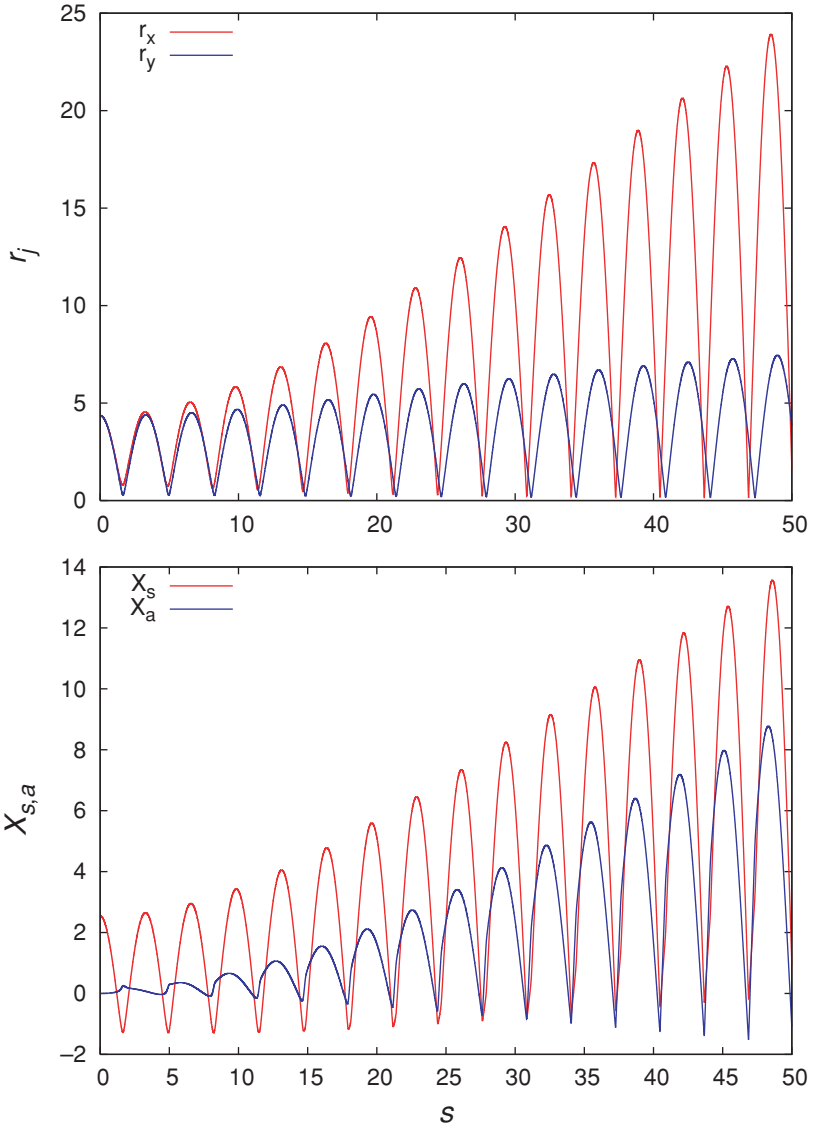

Figure 1. (Colour online) The upper graph shows the evolution of the envelope obtained by direct integration of (2.5). The variables r_x and r_y are represented by the red and blue lines, respectively. The lower graph illustrates the evolution of the oscillation modes of the beam. The variables X_s and X_a are represented by the red and blue lines, respectively.

the emittance coupling, which, thus, result in strong correlations between the particle positions and the transverse momenta. The emittance oscillations are now driven by variations of the space-charge force due to the beam compression and expansion. The rapid emittance oscillations are due to the coherent transverse plasma oscillations in the beam and are an expression of the periodic energy exchange between the potential and the kinetic energy.

https://doi.org/10.1017/S0022377809990419 Published online by Cambridge University Press

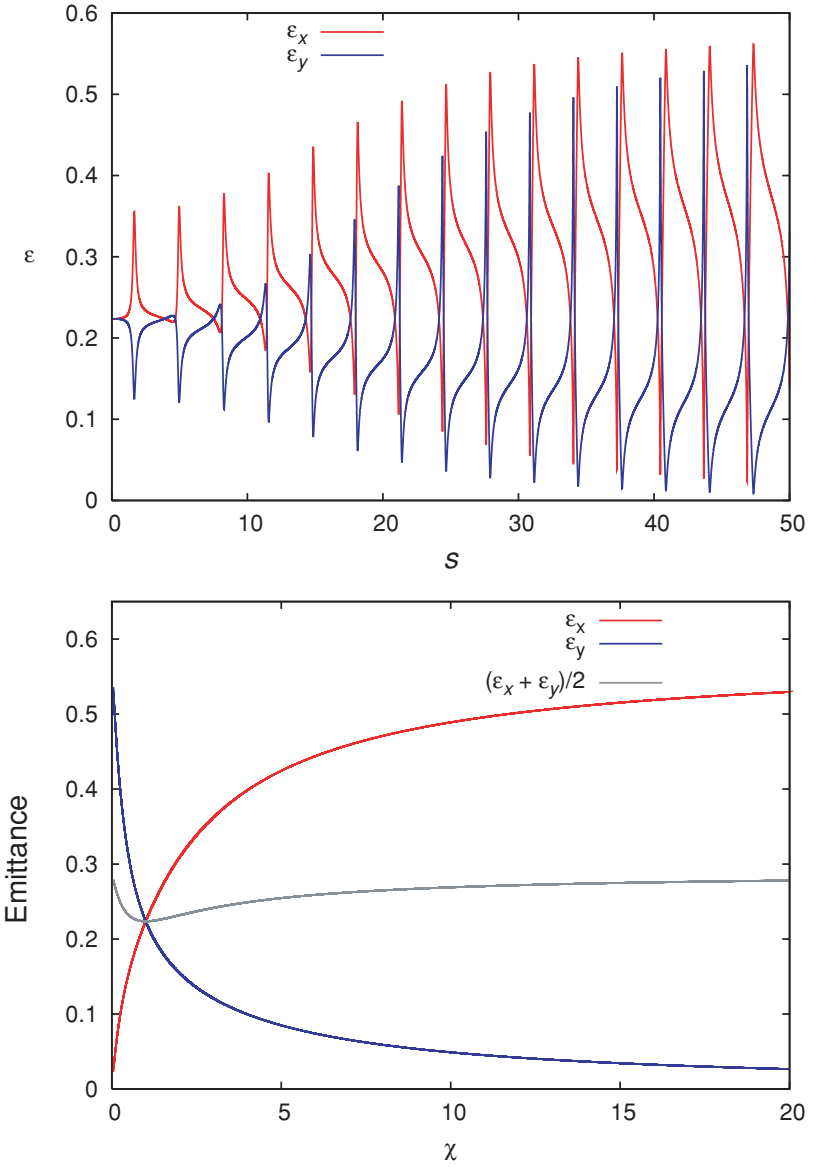

Figure 2. (Colour online) Evolution of the emittance (top) obtained of (2.6) and (2.7). ϵ_x and ϵ_y are represented by red and blue lines, respectively. Emittance and sum transversal emittance (bottom) as a function of the ratio of the envelope beam $\chi = r_x/r_y$. ϵ_x, ϵ_y, and $(\epsilon_x + \epsilon_y)/2$ versus χ are represented by red, blue, and gray lines, respectively. Notice that $(\epsilon_x + \epsilon_y)/2$ shows a much smoother anisotropic variable (χ) response.

In Fig. 2, one also observe an increase in the maximum of emittance oscillations. This effect is a direct consequence of nonlinearities in the particle oscillations around their equilibrium positions. Excess energy is required in order to drive these nonlinearities, which, on their turn, are caused by the energy anisotropy between different degrees of freedom. Figure 2 (bottom) shows ϵ_x and ϵ_y versus the semi-axis

https://doi.org/10.1017/S0022377809990419 Published online by Cambridge University Press

ratio r_x/r_y, where ϵ_x increases and ϵ_y decreases with increasing r_x/r_y but ϵ_y increases and ϵ_x decreases with decreasing r_x/r_y. The fact that ϵ_x increases as the the semi-axis length increases may seem counterintuitive . This effect arises from space charge, which increases as the beam size decreases. This can be explained by remembering that the field components, and therefore the divergence kick in x and y, are insensitive to the envelope, as follows: an elliptical beam with parabolic density present the boundary field's on the minor and major axes are not similar. In this case, we have $E_x = \partial\phi^{in}/\partial x \rightarrow E_x(r_x, 0) = \frac{2q}{\pi\varepsilon_0(r_x+r_y)}[1 - \frac{2+r_y/r_x}{3(1+r_y/r_x)}]$ and $E_y = \partial\phi^{in}/\partial y \rightarrow E_y(0, r_y) = \frac{2q}{\pi\varepsilon_0(r_x+r_y)}[1 - \frac{2r_y/r_x+1}{3(1+r_y/r_x)}]$. It can be seen that although these fields are not exactly equal (except when the beam is round) they usually present comparable magnitudes. However, the emittance is an area in phase space and is essentially the divergence spread multiplied by the spatial extent of the plane in the phase space in which the beam lies on. Therefore, if the divergence kicks are of comparable intensity on both planes, the emittance becomes higher in the plane that presents a larger envelope.

It is noteworthy to mention that space charge is responsible for inducing waves in the beam, a collective effect. These waves are characterized by a plasma frequency, and their effect is observed in the asymptotic evolution of the envelope and emittance, as shown in Fig. 3. The exponential growth of the envelope and the emittance exchange is characterized by an instable tilting mode of the beam in a space-charge-dominated regime [13, 33]. The parabolic distribution is characterized by the appearance of the tilting mode where emittances are periodically exchanged between x and y, similar to a second-order difference resonance driven by skew quadrupoles. This tilting instability on the x and y directions obviously requires some amount of anisotropy. According to previous results by the author [18], breathing mode is excited by the symmetric perturbation only, while the antisymmetric perturbation excites only the quadrupole mode. When anisotropy is also considered, this is not the case. We find a mixture of breathing and quadrupole modes. In the present model both modes are resonant and space charge induces a coherent shift of the resonance conditions $l\omega_x - m\omega_y + \Delta\omega = 0$, since the full ensemble of particles respond to the resonance in a coherent way. Thus, the system may follow two distinct behaviors: when $\Delta\omega = 0$ the beam is not affected by space charge [34], whereas when $\Delta\omega \neq 0$ space-charge effects are observed, activating the tilting mode [35]. In this situation, the majority of the test particles launched along the x- and y-axis inside the beam are in a resonant state. In this model the driving term for this resonance, is not a skew quadrupole as in synchrotrons, but the internal space-charge force caused by the exponentially growing tilting of the beam's cross-section.

Nonlinear resonances may eventually yield RMS emittance growth as more and more particles are launched outside of the core. Therefore, a halo is not generated by a collective effect involving all the core particles, but by formation is the resonant interaction between the particles and the mismatch modes. These resonances enable the transfer of energy excess from one plane to another [16]. It is shown bellow that this exchange occur with the halo formation along one preferential direction.

To understand how halo formation takes place, different beam resonances are investigated. The computed frequencies $\omega_{X_s} = \omega_{X_a} = 2.01334$ for the breathing and the quadrupole modes respectively represent a 1:1 resonance, whereas the Fourier analysis of the test particles shows that 2455 of them obey the resonance condition $\omega_x - \omega_y = 0$, with $\omega_x = \omega_y = 1.05461$ - while the other 45 have $\omega_y = 1.00667$.

https://doi.org/10.1017/S0022377809990419 Published online by Cambridge University Press

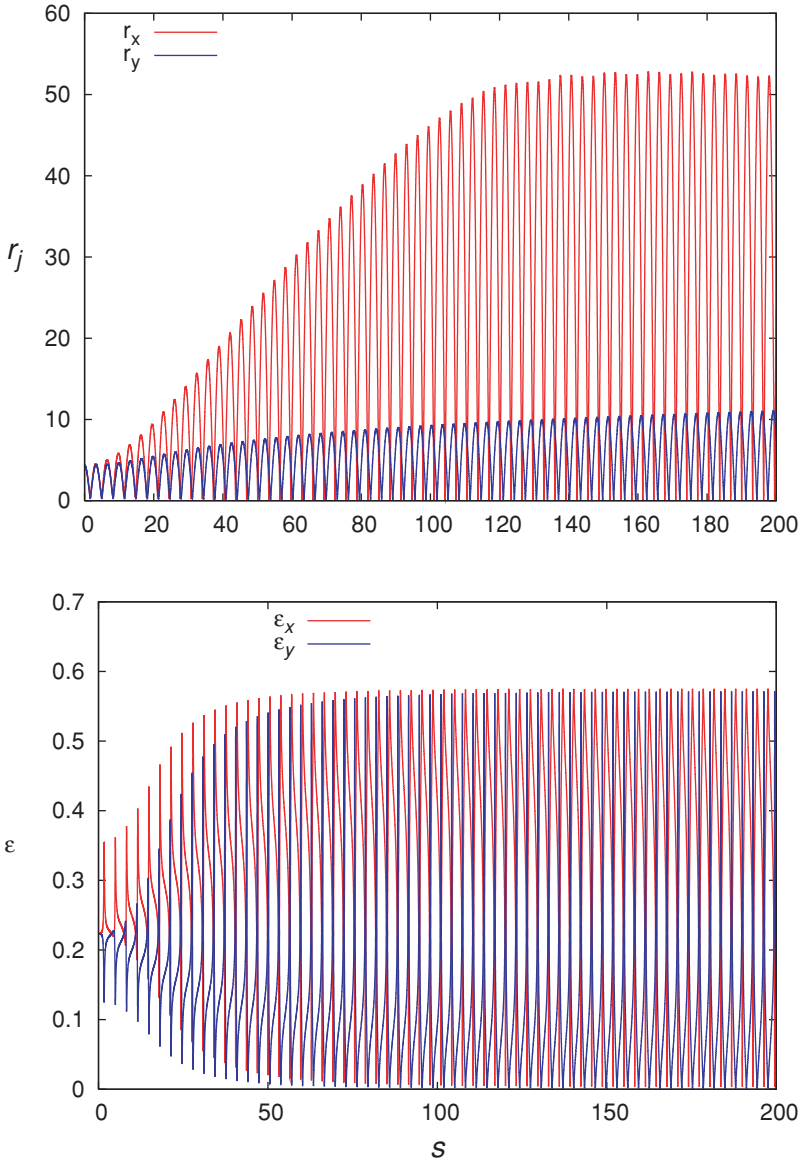

Figure 3. (Colour online) Asymptotic evolution of the envelopes (top) and emittance (bottom) obtained of the (2.5) and, (2.6) and (2.7), respectively. r_x (top), ϵ_x (bottom) and r_y (top) ϵ_y (bottom) are represented by red and blue lines, respectively.

The dominant order of the resonance at $\omega_x/\omega_y = 1$ yields a significant emittance exchange [36]. This creates a barrier between the region inside the beam and the region outside the beam and the space-charge coupling force is responsible for the energy transfer from core oscillations to the single-particle oscillations, yielding 2:1 particle-core resonances in both quadrupole and breathing modes, but only in the y direction of the test particles [15]. As a consequence, the halo formation takes place along the y direction, as illustrated in Fig. 5.

https://doi.org/10.1017/S0022377809990419 Published online by Cambridge University Press

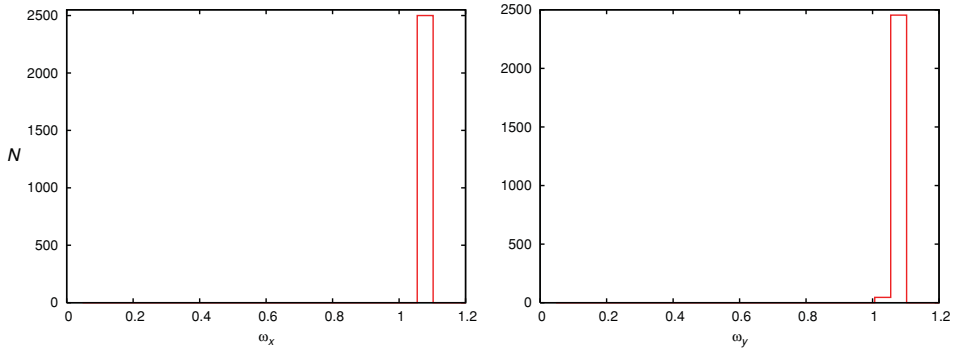

Figure 4. (Colour online) The histogram of the frequencies ω_x and ω_y of 2500 test particles, calculated numerically through the Fourier transform. The test particles were launched along the x- and y-axis in specific regions inside the beam (between $0.01r_x$ and $0.7r_x$ spaced by $0.0004r_x$ along the x direction, and between $0.01r_y$ and $0.7r_y$ spaced by $0.0004r_y$ along the y direction). The values obtained for the frequencies can be found in the text.

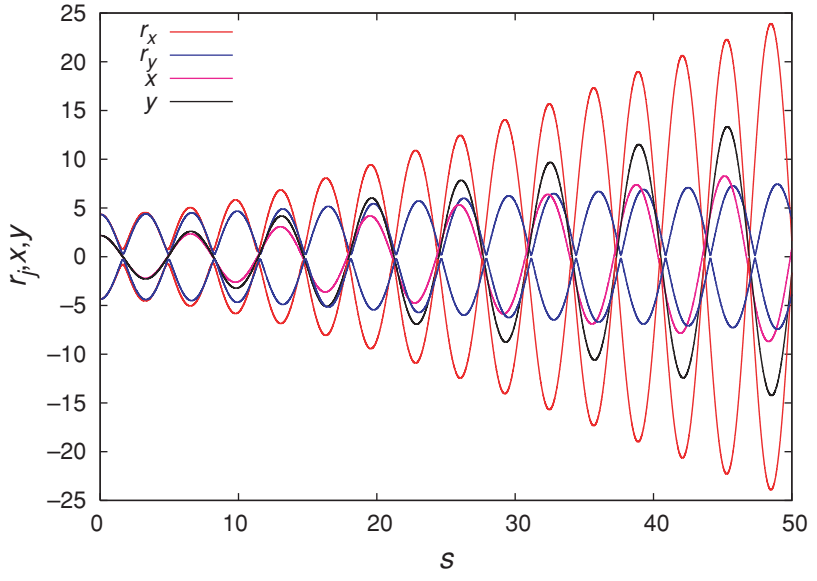

Figure 5. (Colour online) Dynamical evolution of a single test particle. We assumed initially that $x = 0.5r_x$ and $y = 0.5r_y$. The variables x and y of the test particle are represented by black and pink lines, respectively. The evolution of the envelopes r_x and r_y are represented by red and blue lines, respectively.

For a large-size RMS mismatched beam with an initial ratio $\chi = 1$ between the envelopes, the ratio of oscillation energies in the x and y directions, given by $\xi = (r_y\epsilon_x)^2/(r_x\epsilon_y)^2 = 1$ [37, 38], remains constant. This can be explained, since $\xi = \eta^2/\chi^2$ and for our model $\chi = \eta$, following (2.6) and (2.7) and the definitions of the anisotropic variables. As illustrated in Fig. 6, the quantities χ and η vary in a discontinuous way, which characterizes an anisotropic beam [26, 39]. The anisotropy leading to a coupling resonance [40, 41] in the presence of nonlinear

https://doi.org/10.1017/S0022377809990419 Published online by Cambridge University Press

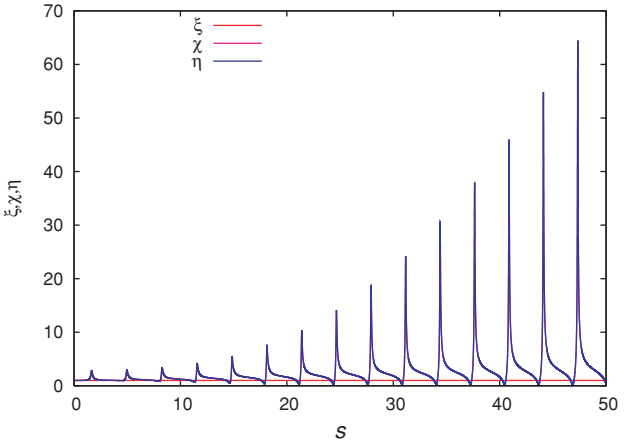

Figure 6. (Colour online) The dynamical evolution of the ratio of oscillation energies ξ and of the anisotropic ratios χ and η. The quantity ξ is represented by the red line, while χ and η are represented by the blue line – χ appears superposed by η.

space-charge forces was suggested as a possible approach to the equipartitioning problem [17, 28, 32], since collisions are not responsible for the energy transfer in linacs. The collective oscillations of the space-charge density is the underlying mechanism of the system, as they create nonlinear forces, similar to those magnetic sextupoles, which lead to the resonant coupling as observed by Kandrup et al. [42].

4. Conclusions

In this paper we examined the anisotropies in the ion beam in a linear focusing channel. The effects of the particle–particle resonances and of the wave-particle resonances in the beam were analyzed. It was shown that these resonances lead to the spatial anisotropization of the beam, that is, the envelope ratio, and therefore the emittance ratio, are different from unity.

The nonlinear space-charge forces lead to the equipartitioning of energy between the degrees of freedom. In space-charge-dominated beams, the Coulomb collisions are not usually responsible for energy transfers. However, it has been shown that space-charge waves are possible candidates to generate coupling between the degrees of freedom [17, 28]. The equipartitioning of an anisotropic beam involves a nonlinear energy transfer and the evolution toward a quasi-equilibrium state, as a consequence of the resonant phase mixing [42, 43]. We used the Fourier transform in order to compute numerically the frequencies, and the frequency of the breathing and quadrupole modes were determined as $\omega_{X_s} = \omega_{X_a} = 2.01334$. The fact that both modes have the same frequency means that are in a resonant state. This core-core resonance is responsible for the elliptical shape of the beam and its increasing size along the x direction [13]. ω_x and ω_y frequencies of 2500 test particles were numerically calculated, resulting in 2455 of them in a resonance condition characterized by $\omega_x - \omega_y = 0$. This is a direct consequence of the emittance coupling. The remaining 45 test particles were observed with an $\omega_y = 1.00667$. The particle-core 2:1 resonances are present in both the quadrupole and the breathing mode of

https://doi.org/10.1017/S0022377809990419 Published online by Cambridge University Press

the core oscillation, only within the y direction of these test particles [15]. Thus, halo formation occurs along the y direction. The anisotropy leading to coupling resonance [40, 41] in the presence of nonlinear space-charge forces was suggested as an approach to the equipartitioning problem [17, 28, 32].

This series of phenomena suggest an direction for future research. We can develop an approach to model locally anisotropic kinetic processes [44]. The generalization of kinetic equations to anisotropics beams is not a trivial task. In order to consider the anisotropic processes of microscopic or macroscopic natures it is necessary to reformulate the kinetic theory in anholonomic frames. The modelling of kinetic processes with respect to anholonomic frames is very useful with the aim of elucidating flows of fluids of particles not in local equilibrium. The deduction of the equation for one-particle distribution function in anisotropics phase-space will be considered in a future work.

Acknowledgements

In memory of my father Wilson Simeoni. The author would like to thanks Conselho Nacional de Desenvolvimento Científico e Tecnológico (CNPq).

References

[1] Lagniel, J. 1994 *Nucl. Instrum. Methods Phys. Res. Sect.* A **345**, 46.
[2] Lagniel, J. 1994 *Nucl. Instrum. Methods Phys. Res. Sect.* A **345**, 405.
[3] Gluckstern, R. L. 1994 *Phys. Rev. Lett.* **73**, 1247.
[4] Jameson, R. 1998 *PAC93 Proc. IEEE*, 3926.
[5] Wangler, T. P., Crandall, K. P., Ryne, R. and Wang, T. S. 1998 *Phys. Rev. ST Accel. Beams* **1**, 084201.
[6] Gluckstern, R. L., Cheng, W. H. and Ye, H. 1995 *Phys. Rev. Lett.* **75**, 2835.
[7] Gluckstern, R. L., Cheng, W. H., Kurennoy, S. and Ye, H. 1996 *Phys. Rev.* E **54**, 6788.
[8] Qian, Q. and Davidson, R. C. 1996 *Phys. Rev.* E **53**, 5349.
[9] Okamoto, H. and Ikegami, M. 1997 *Phys. Rev.* E **55**, 4694.
[10] Ikegami, M. 1999 *Phys. Rev.* E **59**, 2330.
[11] Fedotov, A. V., Hofmann, I., Gluckstern, R. L. and Okamoto, H. 2003 *Phys. Rev. ST Accel. Beams* **6**, 094201.
[12] Montague, B. W. 1968 CERN-Report No. 68–38, CERN.
[13] Hofmann, I. 1998 *Phys. Rev.* E. **57**, 4713.
[14] Fedotov, A. V. 2006 *Nucl. Instrum. Methods Phys. Res. Sect.* A **557**, 216.
[15] Ikegami, M. 1999 *Nucl. Instrum. Methods Phys. Res. Sect.* A **435**, 284.
[16] Hofmann, I., Qiang, J. and Ryne, R. 2001 *Phys. Rev. Lett.* **86**, 2313, Hofmann, I. and Boine-Frankenheim, O. 2001 *Phys. Rev. Lett.* **87**, 034802, Franchetti, G., Hofmann, I. and Jeon, D. 2002 *Phys. Rev. Lett.* **88**, 254802.
[17] Kishek, R. A., O'Shea, P. G. and Reiser, M. 2000 *Phys. Rev. Lett.* **85**, 4514.
[18] Simeoni, W. Jr, Rizzato, F. B. and Pakter, R. 2006 *Phys. Plasmas* **13**, 063104.
[19] Lapostolle, P. M. 1971 *IEEE Trans. Nucl. Sci.* **NS-18**, 1101.
[20] Sacherer, F. J., 1971 *IEEE Trans. Nucl. Sci.* **NS-18**, 1105.
[21] Lapostolle, P. M. 1965 CERN AR/Int. SG/65–27.
[22] Davidson, R. C. and Qin, H. 2001 *Physics of Intense Charged Particle Beams in High Energy Accelerators* 257–299. Singapore: World Scientific.
[23] Lapostolle, P. M., Lombardi, A. and Wangler, T. P. 1993 CERN/PS 93–11 (HI).

[24] Neri, F. and Rangarajan, G. 1990 *Phys. Rev. Lett*. **64**, 1073.
[25] Dragt, A., Neri, F. and Rangarajan, G. 1992 *Phys. Rev.* A **45**, 2572.
[26] Simeoni, W. Jr, 2009 arXiv:0904.3089v1.
[27] Piovella, N., Bourdier, A., Chaix, P. and Iracane, D. 1994 *EPAC94 Proc*., 1186.
[28] Wangler, T. P., Guy, F. W. and Hofmann, I. 1986 *LINAC86 Proc*., 340.
[29] Frigo, M. and Johnson, S. G. 2005 *Proc. IEEE* **93**(2), 216–231.
[30] Hofmann, I., Franchetti, G., Qiang, J. and Ryne, R. D. 2004 *EPAC04 Proc*., 1960.
[31] Ohnuma, S. and Gluckstern, R. L. 1985 *IEEE Trans. Nucl. Sci*. **32**, 2261.
[32] Lagniel, J. M. and Nath, S. 1998 *EPAC98 Proc*., 1118.
[33] Franchetti, G., Hofmann, I. and Aslaninejad, M. 2005 *Phys. Rev. Lett*. **94**, 194801.
[34] Hofmann, I., Franchetti, G. and Boine-Frankenheim, O. 2003 *Phys. Rev. ST Accel. Beams* **6**, 024202.
[35] Aslaninejad, M. and Hofmann, I. 2003 *Phys. Rev. ST Accel. Beams* **6**, 124202.
[36] Hofmann, I. 1997 *PAC97 Proc., IEEE*, 1852.
[37] Jameson, R. A. 1981 *IEEE Trans. Nucl. Sci.* **28**, 2408.
[38] Young, L. M. 1997 *PAC97 Proc*., 1920.
[39] Startsev, E. A., Davidson, R. C. and Qin, H. 2005 *Phys. Rev. ST Accel. Beams* **8**, 124201.
[40] Hofmann, I. 1981 *IEEE Trans. Nucl. Sci.* **28**, 2399.
[41] Hofmann, I. and G. Franchetti, G. 2006 *Phys. Rev. ST Accel. Beams* **9**, 054202.
[42] Kandrup, H. E, Vass, I. M. and Sideris, I. V. 2003 *Mon. Not. R. Astron. Soc*. **341**, 927.
[43] Bohn, C. L. and Sideris, I. V. 2003 *Phys. Rev. ST Accel. Beams* **6**, 034203.
[44] Vacaru, S. I. 2001 *Ann. Physics* **290**, 83.